Spin relaxation in a generic two-dimensional spin-orbit coupled system

Tudor D. Stanescu
Condensed Matter Theory Center, Department of Physics, University of Maryland, College Park, Maryland 20742-4111, USA

Victor Galitski
Condensed Matter Theory Center and Joint Quantum Institute, Department of Physics, University of Maryland, College Park, Maryland 20742-4111, USA

(Received 13 November 2006; published 9 March 2007)

We study the relaxation of a spin density injected into a two-dimensional electron system with generic spin-orbit interactions. Our model includes the Rashba as well as linear and cubic Dresselhaus terms. We explicitly derive a general spin-charge coupled diffusion equation. Spin diffusion is characterized by just two independent dimensionless parameters, γ_R and γ_D, which control the interplay between different spin-orbit couplings. The real-time representation of the diffuson matrix (Green's function of the diffusion equation) is evaluated analytically. The diffuson describes space-time dynamics of the injected spin distribution. We explicitly study two regimes: The first regime corresponds to negligible spin-charge coupling and is characterized by standard charge diffusion decoupled from the spin dynamics. It is shown that there exist several qualitatively different dynamic behaviors of the spin density, which correspond to various domains in the (γ_R, γ_D) parameter space. We discuss in detail a few interesting phenomena such as an enhancement of the spin-relaxation times, real-space oscillatory dynamics, and anisotropic transport. In the second regime, we include the effects of spin-charge coupling. It is shown that the spin-charge coupling leads to an enhancement of the effective charge diffusion coefficient. We also find that in the case of strong spin-charge coupling, the relaxation rates formally become complex and the spin-charge dynamics is characterized by real-time oscillations. These effects are qualitatively similar to those observed in spin-grating experiments [C. P. Weber *et al.*, Nature (London) **437**, 1330 (2005)].

DOI: 10.1103/PhysRevB.75.125307 PACS number(s): 73.21.Fg, 72.25.Dc, 72.25.Rb, 72.10.−d

I. INTRODUCTION

Spin-orbit coupled systems host an amazing variety of interesting effects,[1] which are currently the subject of intense experimental and theoretical investigations. The interest in this field stems from the fact that spin-orbit coupling opens the possibility of controlling the electron spin[2] using purely electrical means[3–8] with potential applications in spintronics[9,10] and quantum computing.[1] The microscopic origin of the spin-orbit interaction in a low-dimensional system is the absence of inversion symmetry in the semiconductor crystal and confining potential. This leads to the appearance of the Rashba and Dresselhaus (linear and cubic) spin-orbit terms in the effective Hamiltonian.[11–14] The spin-orbit interaction results in a variety of macroscopic effects such as antilocalization,[15,16] electric-field-induced spin accumulation,[17,18] spin-galvanic effects,[19] etc.

One particularly important aspect of spin transport in disordered systems is Dyakonov-Perel spin relaxation.[20] The source of this effect is the precession of the electron spin around a momentum-dependent magnetic field. The electron momentum changes randomly due to electron scatterings off of impurities, which, in turn, randomizes spin precession. One should note here that a large spin-relaxation rate is typically considered an undesirable effect from the experimental point of view. On the one hand, the Dyakonov-Perel spin-relaxation rate is proportional to the strength of spin-orbit interactions. On the other hand, the existence of relatively strong spin-orbit interaction is needed for the appearance of nontrivial spin transport.[21,22] It is therefore important to understand the interplay between different phenomena in spin transport and search for possibilities to reduce the negative effects of spin relaxation.

We should mention here that the issue of spin relaxation has been extensively studied in experiments. In particular, Cameron *et al.* and Weber *et al.* have used the transient spin-grating method to study spin dynamics in two-dimensional semiconductor systems.[23–25] This experimental technique is based on optical injection of spin polarized electrons in a two-dimensional quantum well, which generates a spin-density wave with a wave vector in the plane of the two-dimensional system and the spin polarization perpendicular to the plane. Particularly interesting results revealed by these experiments[24] were an enhancement of the charge diffusion coefficient and an unusual time dependence of the spin-grating amplitude, which exhibited oscillatory features in addition to the conventional exponential decay.

Motivated by the aforementioned experimental results, we study theoretically spin transport and spin relaxation in a two-dimensional electron system with generic spin-orbit interaction. We focus our attention on the interplay between different types of spin-orbit couplings and the effects of the spin-charge coupling on the spin-relaxation dynamics. We work within the framework of the diffusion approximation, which assumes that the spin-relaxation length is large compared to the mean free path. We find that depending on the relative values of the Rashba, linear, and cubic Dresselhaus couplings one can have different dynamic spin-relaxation regimes and phenomena such as oscillations of the spin density in real space, anisotropic spin transport, and enhancement of spin-relaxation times. We also study in detail the effect of spin-charge coupling on the diffusive dynamics. We find that

it always leads to a renormalization of the effective charge diffusion coefficient, which gets enhanced compared to the "bare" diffusion constant. We also find that a strong spin-charge coupling may formally lead to a complex spin-relaxation rate and real-time oscillations in the spin and charge diffusion behavior, which are qualitatively similar to the oscillatory behavior observed in experiment. We should note here that the real-time oscillations appear only beyond the formal regime of validity of the diffusion approximation. However, they give a tentative indication that the experimentally observed oscillations may originate from the spin-charge coupling.

Our paper is structured as follows: In Sec. II, we introduce our model Hamiltonian for the noninteracting disordered two-dimensional electron system with spin-orbit interaction and derive a general spin-charge coupled diffusion equation. We introduce natural dimensionless units of length and time and show that in these units, the spin part of the diffusion equation is characterized by two dimensionless parameters, γ_R and γ_D. These parameters are constrained to lie within a circle of radius 2 in the (γ_R, γ_D) parameter space. We also introduce the matrix Green's function of the diffusion equation (diffuson), whose real-time representation describes the spin-relaxation dynamics of interest.

In Sec. III, we consider the spin sector of the diffusion equation (which is justified if the spin-charge coupling is relatively small). We focus our attention on the diagonal z component of the diffuson, which describes the dynamics of injected out-of-plane spin density. We show that there exist different domains in the (γ_R, γ_D)-parameter space, which correspond to qualitatively different dynamic regimes. We explicitly derive the real space-time behavior of the diagonal component of the diffuson matrix in various regimes. We also discuss the spin dynamics as a function of momentum and derive the spin-relaxation spectrum as a function of spin-orbit coupling parameters. In particular, we study in detail the "symmetry point" in the parameter space $(\gamma_R = \gamma_D)$, when the relaxation time becomes infinite in certain directions. We study the behavior of the spin-relaxation spectrum in the vicinity of the symmetry point.

In Sec. IV, we discuss the effects of spin-charge coupling on the spin-relaxation spectrum. We show that the spin-charge coupling may formally lead to a complex spin-relaxation rate, which physically translates into an oscillatory behavior of the spin density. We discuss the validity of the diffusion equation approximation and the implication of our results for understanding spin transport experiments. Our conclusions and a discussion of several open questions are presented in the last, Sec. V.

II. THE DIFFUSION EQUATION

In this section, we introduce the model and derive a general form of the spin-charge coupled diffusion equation. The main results of this section are Eqs. (11) and (13) representing the most general form of the diffusion equation in an electron system with arbitrary spin-orbit interaction. In this and subsequent sections, we use the units $\hbar = k_B = 1$.

We start with the following Hamiltonian, which describes the conduction-band electrons in a III-V-type semiconductor quantum well grown in the [001] direction (set as the z axis):

$$H = \frac{\mathbf{p}^2}{2m} + \mathbf{h}(\mathbf{p}) \cdot \hat{\sigma}, \tag{1}$$

where m is the effective electron mass, $\hat{\boldsymbol{\sigma}} = (\hat{\sigma}_x, \hat{\sigma}_y, \hat{\sigma}_z)$ is the Pauli matrix, and $\mathbf{h}(\mathbf{p}) = (h_x, h_y, h_z)$ are functions of the two-dimensional momentum $\mathbf{p}$ describing the spin-orbit interaction. We assume that the noninteracting electrons are in the presence of a short-range impurity potential, and we investigate the role of the spin-orbit interaction in the coupled spin and charge transport using the diffusion approximation. In general, the second term of the Hamiltonian (1), which describes the spin-orbit interaction, contains both Rashba and Dresselhaus contributions. The Rashba interaction,[11,12] which is due to the inversion asymmetry of the quantum well confining potential, has the form

$$\mathbf{h}^R(\mathbf{p}) = \alpha v_F (p_y, -p_x), \tag{2}$$

where v_F is the Fermi velocity and α is a dimensionless coupling constant. Throughout this work, we will assume that the spin-orbit coupling energy is much smaller than the Fermi energy, i.e., $|\alpha| \ll 1$. Consequently, we will neglect the change of the Fermi surface due to the presence of spin-orbit interaction. We notice that Eq. (2) may also describe the coupling of spin to off-diagonal strain.[5,26,27] The Dresselhaus spin-orbit coupling,[13] arising from the lack of inversion symmetry of the semiconductor crystal, contains terms both linear and cubic in $\mathbf{p}$,

$$\mathbf{h}^{D_1}(\mathbf{p}) = \beta_1 v_F (p_x, -p_y), \tag{3}$$

$$\mathbf{h}^{D_3}(\mathbf{p}) = -4\beta_3 \frac{v_F}{p_F^2} (p_x p_y^2, -p_y p_x^2), \tag{4}$$

where β_1 and β_3 are dimensionless coupling constants with $|\beta_j| \ll 1$, and $p_F = m v_F$ is the Fermi momentum.

In the presence of disorder, the complete description of the coupled spin and charge diffusive transport at long length scales compared to the mean free path is given by a set of linear differential equations that, in its most general form, can be written as

$$\left(\frac{\partial}{\partial t} - \mathcal{D}\boldsymbol{\nabla}^2 \right) \rho_i = (-\Gamma^{ij} + P^{ijm}\nabla_m + \mathbf{C}^{ij}\boldsymbol{\nabla})\rho_j, \tag{5}$$

where $\partial/\partial t$ represents the time derivative, ρ_0 is the charge density, while $\rho_1 = \rho_x$, $\rho_2 = \rho_y$, and $\rho_3 = \rho_z$ are the densities of the corresponding spin components. In Eq. (5), $\mathcal{D}$ represents the diffusion constant and can be expressed in terms of the mean scattering time τ as $\mathcal{D} = \tau v_F^2/2$, $\Gamma^{ij} = (1/\tau_s)_{ij}$ describes the Dyakonov-Perel spin relaxation,[20] P^{ijm} is responsible for the precession of the inhomogeneous spin polarization, and the last term, having nonzero elements $\mathbf{C}^{i0} = \mathbf{C}^{0i}$, describes the spin-orbit mixing of spin and charge degrees of freedom. For convenience, throughout this paper we will express times in units of spin-relaxation time τ_s and lengths in units of spin-relaxation length L_s, unless otherwise stated. The quantities τ_s and L_s depend explicitly on the parameters of the two-dimensional electron system,

$$L_s = \frac{1}{2k_F[\alpha^2 + (\beta_1 - \beta_3)^2 + \beta_3^2]^{1/2}}, \tag{6}$$

$$\tau_s = \frac{2\tau}{g^2[\alpha^2 + (\beta_1 - \beta_3)^2 + \beta_3^2]}, \tag{7}$$

where $g = 2v_F k_F \tau$ is a coefficient proportional to the dimensionless conductance. Using the units (6) and (7), we can write the coefficients from Eq. (5) as dimensionless coupling constants. For example, the diagonal contributions to the spin-relaxation terms are $\Gamma_{xx} = \Gamma_{yy} = 1$ and $\Gamma_{zz} = 2$. The final matter of convenience concerns the parametrization of the spin-orbit interaction. This interaction can be described in terms of the original coupling constants $(\alpha, \beta_1, \beta_3)$ or, alternatively, in terms of a new set of parameters, $(\Gamma, \gamma_R, \gamma_D)$, defined by

$$\Gamma^2 = \alpha^2 + \beta_1^2 + \beta_3^2,$$

$$\gamma_R = \frac{2\alpha}{\sqrt{\alpha^2 + (\beta_1 - \beta_3)^2 + \beta_3^2}}, \quad \gamma_D = \frac{2(\beta_1 - \beta_3)}{\sqrt{\alpha^2 + (\beta_1 - \beta_3)^2 + \beta_3^2}}. \tag{8}$$

The parameter Γ represents a measure of the overall strength of the spin-orbit interaction, while γ_R and γ_D characterize the interplay between the Rashba and Dresselhaus contributions. By convention, the sign of Γ is the same as the sign of β_3. We derive the diffusion equations using the standard density-matrix formalism,[28] used previously in Refs. 29–32. Equation (5) can by rewritten in the form

$$(\delta_{ij} - \Pi_{ij})\rho_j = 0, \tag{9}$$

where, for a homogeneous system, $\delta_{ij} - \Pi_{ij}(\omega, \mathbf{k}) = (-i\omega + k^2)\delta_{ij} + \Gamma^{ij} + P^{ijm}k_m + \mathbf{C}^{ij}\mathbf{k}$ and summations over repeated indices are assumed. The matrix $\hat{\Pi}$ represents the kernel of the diffusion equation and can be expressed in terms of retarded and advanced Green's functions as

$$\hat{\Pi}_{ij}(\omega, \mathbf{k}) = \frac{1}{4\pi\nu_F\tau}\int \frac{d^2\mathbf{q}}{(2\pi)^2}\mathrm{Tr}\{\hat{\sigma}_i\hat{G}^R(\omega/2, \mathbf{k} + \mathbf{q}/2) \times \hat{\sigma}_j\hat{G}^A(\omega/2, \mathbf{k} - \mathbf{q}/2)\}, \tag{10}$$

where $\hat{G}^{R(A)}$ is the 2×2 retarded (advanced) Green's function matrix averaged over disorder, $\hat{\sigma}_i$ are the Pauli matrices, ν_F is the density of states at the Fermi energy and $\mathrm{Tr}\{\cdots\}$ involves the trace over spin indices. The diffusion approximation represents the low-frequency, long-wavelength limit of Eq. (10). This approximation is valid as long as the scattering time is much shorter than the spin precession time; i.e., in the weak spin-orbit coupling limit, $\Gamma v_F k_F \tau \ll 1$. Taking the appropriate small frequency and small momentum limit, we obtain

$$\hat{1} - \hat{\Pi}(\omega, \mathbf{k}) = \begin{pmatrix} s-1 & -ig(\mu_0 k_x + \mu_1 k_y) & ig(\mu_1 k_x + \mu_0 k_y) & 0 \\ -ig(\mu_0 k_x + \mu_1 k_y) & s & \frac{1}{2}\gamma_R\gamma_D & -i(\gamma_R k_x + \gamma_D k_y) \\ ig(\mu_1 k_x + \mu_0 k_y) & \frac{1}{2}\gamma_R\gamma_D & s & -i(\gamma_D k_x + \gamma_R k_y) \\ 0 & i(\gamma_R k_x + \gamma_D k_y) & i(\gamma_D k_x + \gamma_R k_y) & s+1 \end{pmatrix}, \tag{11}$$

where $\hat{1}$ is the 4×4 unit matrix, $s = -i\omega + k^2 + 1$, and the spin-charge coupling is characterized by the parameters

$$\mu_0 = \frac{(3\beta_3 - \beta_1)(\alpha^2 - \beta_1^2 + \beta_3^2) - \beta_1\beta_3^3}{\sqrt{\alpha^2 + (\beta_1 - \beta_3)^2 + \beta_3^2}},$$

$$\mu_1 = \frac{\alpha(\alpha^2 - \beta_1^2 + 6\beta_3^2)}{\sqrt{\alpha^2 + (\beta_1 - \beta_3)^2 + \beta_3^2}}. \tag{12}$$

In addition, it will be convenient to consider the diffusion problem within a coordinate system that is rotated in the x-y plane counterclockwise with $\pi/2$ relative to the initial coordinate system.[35] The rotated coordinates are $r_+ = (y+x)/\sqrt{2}$ and $r_- = (y-x)/\sqrt{2}$, while the new components of the spin density will be $\rho_+ = (\rho_y + \rho_x)/\sqrt{2}$ and $\rho_- = (\rho_y - \rho_x)/\sqrt{2}$, in addition to ρ_z and the charge density ρ_0 that remain unchanged. Relative to the rotated coordinate system, diffusion is described by the operator

$$\hat{1} - \hat{\Pi}^{(r)}(\omega, \mathbf{k}) = \begin{pmatrix} s-1 & i\xi(\mu_0 - \mu_1)k_- & i\xi(\mu_0 + \mu_1)k_+ & 0 \\ i\xi(\mu_0 - \mu_1)k_- & s + \frac{1}{2}\gamma_R\gamma_D & 0 & -i(\gamma_R + \gamma_D)k_+ \\ i\xi(\mu_0 + \mu_1)k_+ & 0 & s - \frac{1}{2}\gamma_R\gamma_D & -i(\gamma_R - \gamma_D)k_- \\ 0 & i(\gamma_R + \gamma_D)k_+ & i(\gamma_R - \gamma_D)k_- & s+1 \end{pmatrix}, \tag{13}$$

where the four columns correspond to ρ_0, ρ_+, ρ_-, and ρ_z, respectively. Equations (11) and (13) are the main results of this section.

The physical problem that we will be solving on the basis of Eqs. (11) and (13) is to describe the transport of an injected spin density in the presence of a general type of spin-orbit coupling. Assuming that a spin (or charge) density with components $\rho_i(0,\mathbf{r})$ was injected into the system at $t=0$, the density profile at times $t>0$ will be

$$\rho_i(t,\mathbf{r}) = \int dr' D_{ij}(t,\mathbf{r},\mathbf{r}')\rho_j(0,\mathbf{r}'), \tag{14}$$

where $\hat{D}$ is the diffuson, i.e., the Green's function of the diffusion equation. The physical meaning of the diffuson can be understood if we assume that initially we inject a δ-like, density profile $\rho_j(0,\mathbf{r})=\delta(\mathbf{r})$. The spin and charge densities at any later time are given by the matrix elements of the diffuson, $\rho_i(t,\mathbf{r})=D_{ij}(t,\mathbf{r})$. For a homogeneous system, the diffuson is the inverse of the diffusion kernel,

$$\hat{D} = [\hat{1} - \hat{\Pi}]^{-1}. \tag{15}$$

Consequently, solving the transport problem for an injected spin density implies inverting the matrix in Eq. (11) or (13) and performing the appropriate Fourier transforms. We notice that the spin and charge dynamics is controlled by the poles of $\hat{D}(\omega,\mathbf{k})$. These poles determine four relaxation modes $i\omega_\alpha(\mathbf{k})=1/\tau_\alpha(\mathbf{k})$, which follow from the equation

$$\Delta(\omega,\mathbf{k}) \equiv \det[\hat{1} - \hat{\Pi}(s,\mathbf{k})] = 0. \tag{16}$$

A time dependent matrix element of the diffuson can be written, in general, as

$$\mathrm{D}_{ij}(t,\mathbf{k}) = \sum_{l=0}^{3} A_l(\mathbf{k}) e^{-i\omega_l(\mathbf{k})t}, \tag{17}$$

where the amplitudes $A_l(\mathbf{k})$ are functions of momentum. We should emphasize here that the long-time relaxation of the injected spin density is uniquely determined by the lowest minimum of the relaxation rate modes. In a standard diffusion problem, the charge relaxation rate is $1/\tau_0(\mathbf{k})=\mathcal{D}k^2$ (where $\mathcal{D}$ is the diffusion constant, which is equal to 1 in our special units) and the minimum obviously corresponds to $\mathbf{k}=\mathbf{0}$. By contrast, in the presence of spin-orbit interaction, the k dependence of the relaxation rate is more complicated, with possible minima at finite momenta. The detailed dependence of the relaxation rate on the spin-orbit interaction is analyzed in the following sections.

III. THE SOLUTION OF THE TIME-DEPENDENT DIFFUSION EQUATION: THE SPIN SECTOR

In this section, we discuss the spin-relaxation spectrum and derive the diffuson in momentum space (Sec. III A) and real space (Sec. III B). The main results of Sec. III A are Eqs. (21) and (26), describing the spin-relaxation spectrum, and Fig. 1, which summarizes the properties of the spectrum. The behavior in the vicinity of the symmetry points characterized by an infinite spin-relaxation time is illustrated in Fig. 2. Equations (30), (33), and (34) describe spin diffusion in real space.

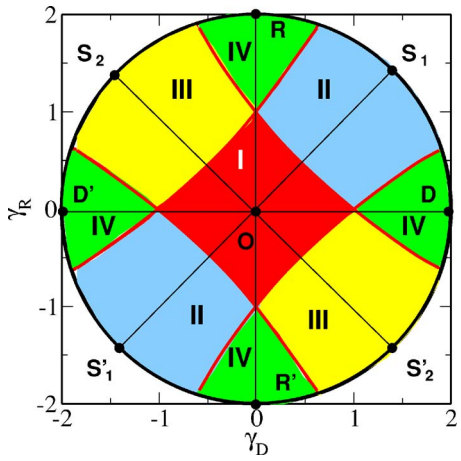

FIG. 1. (Color online) Diagram summarizing the the types of minima characterizing the lowest-energy relaxation rate modes $i\omega_1$ and $i\omega_2$ [see Eq. (21)]. The spin sector is uniquely described by the dimensionless spin-orbit coupling constants γ_R and γ_D. These parameters are proportional to the Rashba interaction and to the difference between the linear and cubic Dresselhaus couplings, respectively, and they satisfy the physical constraint $\gamma_R^2+\gamma_D^2\leqslant 4$ [see Eq. (8)]. In the central red zone (region I), both modes $i\omega_1$ and $i\omega_2$ have the minimum at $\mathbf{k}=0$. In the blue zone II (yellow zone III), the minimum of the $i\omega_1$ ($i\omega_2$) mode is at zero momentum, while the minimum of the $i\omega_2$ ($i\omega_1$) mode is at a finite wave vector k_+^0 (k_-^0) given by Eq. (23). In the green domains IV, both modes have a finite k-vector minimum at k_-^0 (for $i\omega_1$) and k_+^0 (for $i\omega_2$). The points R and R' correspond to the pure Rashba case $(\gamma_R,\gamma_D)=(\pm 2,0)$, while the segment DD' corresponds to the pure Dresselhaus spin-orbit interaction, $\gamma_R=0$, $\gamma_D\in[-2,2]$. At the end points $\gamma_D=\pm 2$, the cubic Dresselhaus term vanishes. The spin dynamics is isotropic for $\gamma_R\gamma_D=0$, i.e., along the RR' and $D'D$ segments. S_j and S_j' are special symmetry points characterized by a zero minimum relaxation rate $i\omega_j(k^0)$, i.e., an infinite spin- relaxation time.

A. Momentum space picture

The diffusion approximation leading to Eq. (11) is rigourously valid only in the weak spin-orbit coupling regime characterized by $\Gamma v_F k_F \tau \ll 1$. In this limit, the spin-charge coupling is small, $g|\mu_{1,2}|\ll 1$, and can be neglected in the leading approximation. The goal of this section is to determine the role played by the interference between different spin-orbit interaction terms in spin diffusion. In particular, motivated by experiments that probe spin dynamics optically, we concentrate on the properties of the out-of-plane component of the spin density. To address this problem, we have to determine the element $D_{zz}=[\hat{1}-\hat{\Pi}^{-1}]_{zz}$ of the Green's function for the diffusion equation (the diffuson). The general expression for the diagonal z component of the diffuson in the absence of spin-charge coupling is

$$D_{zz}(s,\mathbf{k}) = [s^2 - (\gamma_R\gamma_D/2)^2]/\Delta(s,\mathbf{k}),$$

where $\Delta(s,\mathbf{k})$ is a third-order polynomial in s,

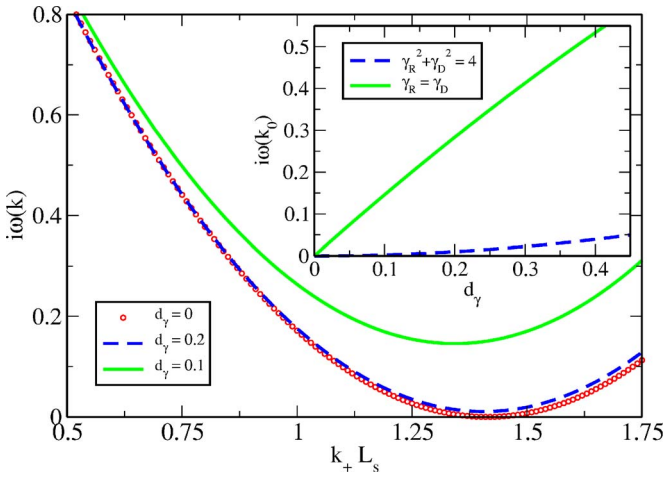

FIG. 2. (Color online) Momentum dependence of the relaxation rate mode $i\omega_2(k_+)$ for spin-orbit coupling parameters in the vicinity of the symmetry point $\gamma_R=\gamma_D=\sqrt{2}$ (point S_1 in Fig. 1). In this regime, the $i\omega_2$ mode has a finite wave-vector minimum along the k_+ direction. At the symmetry point, the dispersion curve becomes gapless (red circles), meaning that the spin-relaxation time at $k_+^0=\sqrt{2}/L_s$ is infinite. As we depart from the symmetry point, a finite gap opens. The spin-orbit coupling parameters for the blue dashed curve correspond to a point on the RS_1D arc in Fig. 1, while the green (light gray) curve is for a point on the S_1O segment, both points being in the vicinity of S_1. The gap size as a function of the distance d_γ from the symmetry point [see Eq. (21) for the definition of d_γ] is shown in the inset. The blue dashed curve corresponds to a spin-orbit interaction with vanishing cubic Dresselhaus contribution $\beta_3=0$ (the RS_1D arc), while the green (light gray) curve was obtained for $\gamma_R=\gamma_D<\sqrt{2}$ (the S_1O segment). To observe a substantial enhancement of the spin-relaxation time at finite momentum, i.e., to have a small gap in the relaxation rate curve, the cubic Dresselhaus spin-orbit interaction β_3 should be minimal.

$$\Delta(s,\mathbf{k})=s^2(s+1)-s\left[(\gamma_R^2+\gamma_D^2)k^2+4\gamma_R\gamma_D k_x k_y+\left(\frac{\gamma_R\gamma_D}{2}\right)^2\right]+\gamma_R^2\gamma_D^2k^2+\gamma_R\gamma_D(\gamma_R^2+\gamma_D^2)k_xk_y-\left(\frac{\gamma_R\gamma_D}{2}\right)^2. \quad (18)$$

The spin dynamics is determined by the three spin-relaxation rate modes, $i\omega_j(\mathbf{k})=-s_j(\mathbf{k})+k^2+1$, obtained by solving the equation $\Delta(s,\mathbf{k})=0$. For later reference, let us identify the modes that control the spin dynamics, together with the charge mode, according to their zero momentum values,

$$i\omega_0(0)=0,$$

$$i\omega_1(0)=1-\frac{\gamma_R\gamma_D}{2},$$

$$i\omega_2(0)=1+\frac{\gamma_R\gamma_D}{2},$$

$$i\omega_3(0)=2, \quad (19)$$

where the mode $i\omega_0$ is responsible for charge diffusion and has the standard form $i\omega_0(\mathbf{k})=k^2$ if we neglect spin-charge coupling. Let us first focus on the experimentally relevant special case of momentum parallel to the [110] or [1$\bar{1}$0] directions corresponding to $k_\pm$. Inverting the matrix from Eq. (13), we obtain

$$D_{zz}(s,k_\pm)=\frac{s\pm\frac{\gamma_R\gamma_D}{2}}{s^2+s\left(1\pm\frac{\gamma_R\gamma_D}{2}\right)-k_\pm^2(\gamma_R\pm\gamma_D)^2\pm\frac{\gamma_R\gamma_D}{2}}. \quad (20)$$

Notice that for k vectors oriented along these special directions, one of the modes $i\omega_1$ or $i\omega_2$ does not contribute to the dynamics and, consequently, the problem simplifies significantly. The time dependence of D_{zz} can be obtained by Fourier transforming Eq. (20) with respect to the frequency. This time dependence is uniquely determined by the roots of the secular equation $\Delta(s,k_\pm)=0$, i.e., by

$$i\omega_1(k_-)=\frac{3}{2}+k_-^2-\frac{\gamma_R\gamma_D}{4}-\frac{1}{2}\sqrt{\left(1+\frac{\gamma_R\gamma_D}{2}\right)^2+4k_-^2(\gamma_R-\gamma_D)^2},$$

$$i\omega_2(k_+)=\frac{3}{2}+k_+^2+\frac{\gamma_R\gamma_D}{4}-\frac{1}{2}\sqrt{\left(1-\frac{\gamma_R\gamma_D}{2}\right)^2+4k_+^2(\gamma_R+\gamma_D)^2},$$

$$i\omega_3(k_\pm)=\frac{3}{2}+k_\pm^2\pm\frac{\gamma_R\gamma_D}{4}+\frac{1}{2}\sqrt{\left(1\mp\frac{\gamma_R\gamma_D}{2}\right)^2+4k_\pm^2(a_R\pm\gamma_D)^2}. \quad (21)$$

As mentioned above, the modes $i\omega_1(k_+)=1+k_+^2-\gamma_R\gamma_D/2$ and $i\omega_2(k_-)=1+k_-^2+\gamma_R\gamma_D/2$ do not contribute to the dynamics of the out-of-plane component of the spin. The explicit time dependence of D_{zz} for k vectors along the "+" direction is

$$D_{zz}(t,k_+)=\frac{1}{2}[e^{-i\omega_2(k_+)t}+e^{-i\omega_3(k_+)t}]-\frac{\left(1-\frac{\gamma_R\gamma_D}{2}\right)}{2\sqrt{\left(1-\frac{\gamma_R\gamma_D}{2}\right)^2+4k_+^2(\gamma_R+\gamma_D)^2}}[e^{-i\omega_2(k_+)t}-e^{-i\omega_3(k_+)t}]. \quad (22)$$

A similar expression can be obtained for $D_{zz}(t,k_-)$ by replacing k_+ with k_- and $i\omega_2$ with $i\omega_1$ and by changing the sign of γ_D. The spin dynamics at large times, $t\gg\tau_s$, is controlled by the minima of the relaxation rate modes $i\omega_j(k_\pm)$. The mode $i\omega_3$ has always the minimum at $k=0$, $i\omega_3(0)=2$. On the other hand, the position and the values of the minima for the other two modes depend on the spin-orbit coupling parameters.

The mode $i\omega_1$ has a minimum $i\omega_1(0)=1-\gamma_R\gamma_D/2$ at zero wave vector if $\gamma_R^2+\gamma_D^2-5\gamma_R\gamma_D/2<1$. Otherwise, the dispersion curve has a local maximum at $k=0$ and the minimum occurs at a finite wave vector k_-^0. Similarly, the mode $i\omega_2$ has either a zero wave-vector minimum, if $\gamma_R^2+\gamma_D^2+5\gamma_R\gamma_D/2<1$, or otherwise a finite k-vector minimum at k_+^0. The finite wave vectors that describe the positions of the minima are

$$|k_\pm^0|=\frac{\sqrt{(\gamma_R\pm\gamma_D)^4-\left(1\mp\frac{\gamma_R\gamma_D}{2}\right)^2}}{2|\gamma_R\pm\gamma_D|}, \tag{23}$$

while the frequencies corresponding to the minima in the dispersion curves are

$$i\omega_1(k_-^0)=\frac{3}{2}-\frac{\gamma_R\gamma_D}{4}-\frac{\left(1+\frac{\gamma_R\gamma_D}{2}\right)^2}{4(\gamma_R-\gamma_D)^2}-\frac{(\gamma_R-\gamma_D)^2}{4},$$

$$i\omega_2(k_+^0)=\frac{3}{2}+\frac{\gamma_R\gamma_D}{4}-\frac{\left(1-\frac{\gamma_R\gamma_D}{2}\right)^2}{4(\gamma_R+\gamma_D)^2}-\frac{(\gamma_R+\gamma_D)^2}{4}. \tag{24}$$

A summary of the conditions necessary for the existence of these minima in terms of the spin-orbit coupling parameters γ_R and γ_D is presented in Fig. 1. In the red domain (the central zone I), the condition $\gamma_R^2+\gamma_D^2\pm5\gamma_R\gamma_D/2<1$ is satisfied and all the dispersion curves have minima at zero momentum. The blue regions (II) are characterized by a finite wave-vector minimum of the $i\omega_2$ mode along the k_+ direction and a zero momentum minimum of the $i\omega_1$ mode, while the yellow sectors (III) correspond to the $[i\omega_1(k_-^0), i\omega_2(0)]$ pair of minima. Finally, in the green regions (IV) both modes, $i\omega_1$ and $i\omega_2$, have finite k-vector minima corresponding to k_-^0 and k_+^0, respectively. Notice that spin diffusion is isotropic only if $\gamma_R\gamma_D=0$, i.e., for pure Rashba spin-orbit interaction [$\beta_1=\beta_3=0$ or $(\gamma_R,\gamma_D)=(\pm2,0)$, the points R and $R\prime$ in Fig. 1], pure Dresselhaus spin-orbit coupling ($\alpha=0$ or $\gamma_R=0$, the segment $D\prime D$ in Fig. 1), or a combination of Rasba and Dresselhaus contributions with the linear and cubic Dresselhaus terms being equal ($\beta_1=\beta_3$ or $\gamma_D=0$ and $\alpha\neq0$, the segment $RR\prime$ without the end points). In all the other cases, the spin diffuses anisotropically as a result of the interference between the spin-orbit coupling terms.

To be more specific, let us now consider the case $\gamma_R>0$, $\gamma_D>0$, i.e., the quarter defined by the points R, O, and D in Fig. 1. We assume that a uniform out-of-plane spin density was injected into the system and ask about its time evolution. The answer can be obtained using Eq. (22) for $k_+=0$. For a uniform system, the out-of-plane spin diffusion equation that takes the trivial form $D_{zz}(t,0)=\exp(-2t)$, which corresponds to $i\omega_3(0)=2$, represents the uniform spin-relaxation rate of the S_z component. If we consider now the limit of small nonzero momenta and expand all the quantities up to second-order terms in k, we obtain

$$D_{zz}(t,\mathbf{k})\approx\frac{(\gamma_R-\gamma_D)^2}{\left(1+\frac{\gamma_R\gamma_D}{2}\right)^2}k_-^2e^{-i\omega_1(\mathbf{k})t}+\frac{(\gamma_R+\gamma_D)^2}{\left(1-\frac{\gamma_R\gamma_D}{2}\right)^2}k_+^2e^{-i\omega_2(\mathbf{k})t}+e^{-i\omega_3(\mathbf{k})t}, \tag{25}$$

where the dispersion relations at small k vectors take the form

$$i\omega_1(\mathbf{k})\approx i\omega_1(0)+k^2-\frac{(\gamma_R-\gamma_D)^2}{1+\frac{\gamma_R\gamma_D}{2}}k_-^2,$$

$$i\omega_2(\mathbf{k})\approx i\omega_2(0)+k^2-\frac{(\gamma_R+\gamma_D)^2}{1-\frac{\gamma_R\gamma_D}{2}}k_+^2,$$

$$i\omega_3(\mathbf{k})\approx i\omega_3(0)+k^2+\frac{(\gamma_R-\gamma_D)^2}{1+\frac{\gamma_R\gamma_D}{2}}k_-^2+\frac{(\gamma_R+\gamma_D)^2}{1-\frac{\gamma_R\gamma_D}{2}}k_+^2, \tag{26}$$

where $k^2=k_x^2+k_y^2=k_+^2+k_-^2$. The initial decay of the spin density is dominated by the third term in Eq. (25) that has the form $\exp[-(2+D_+k_+^2+\mathcal{D}_-K_-^2)t]$. Here, $\mathcal{D}_\pm$ are effective diffusion constants along the $k_\pm$ directions. This result shows explicitly that the diffusion of the out-of-plane component of the spin is, in general, anisotropic, and that the anisotropy increases rapidly as we approach the symmetry point S_1. Another consequence of these relations is that the asymptotic behavior at $t\gg\tau_s$ is controlled by the $i\omega_1$ mode, unlike the uniform case described solely by $i\omega_3$. In the isotropic case, the relaxation times corresponding to these modes differ by a factor of 2, $\tau_1/\tau_3=i\omega_3/i\omega_1=2$. As we approach the symmetry point, this ratio diverges, $\tau_1/\tau_3=4/(2-\gamma_R\gamma_D)$. At the same time, the prefactor of the first term in Eq. (25) vanishes as we approach the OS_1 line (see Fig. 1) characterized by equal Rashba and Dresselhaus couplings, or if the wave vector is oriented along the k_+ direction. We conclude that, in general, the asymptotic spin relaxation at small (but not-vanishing) k vectors differs strongly from the spin relaxation at $k=0$. In addition, the small wave-vector behavior is, in general, anisotropic as a result of the interference between different spin-orbit coupling terms.

Next, we focus on the finite momentum minima of the dispersion relations (23) and (24). The existence of these minima for the $i\omega_1$ and $i\omega_2$ modes implies an increase in the spin lifetime relative to $k=0$ for the corresponding mode by a factor $i\omega_{1(2)}(0)/i\omega_{1(2)}(k_\mp^0)$. For example, in the pure Rashba case we obtain $k_\pm^0=\sqrt{15}/4$ in units of $1/L_s$, or $k_\pm^0=\alpha k_F\sqrt{15}/2$ in standard units, and an increase in the lifetime by a factor of 16/7, in agreement with previous calculation[29,33] based on the Rashba model.

Another important special case is represented by the symmetry points characterized by equal Rashba and Dresselhaus couplings, more precisely defined by $|\gamma_R|=|\gamma_D|=\sqrt{2}$ (the S_j points in Fig. 1). At a symmetry point, the minimum in the dispersion curve vanishes, $i\omega_{2(1)}(\sqrt{2})=0$, reflecting the ab-

sence of spin relaxation[34,35] at the corresponding wave vector, $k_+^0=\sqrt{2}$ (or $k_-^0=\sqrt{2}$ if $\gamma_R\gamma_D<0$). The existence of a finite k-vector minimum in the dispersion curves is illustrated in Fig. 2. The red curve with small circles corresponds to the symmetry point $\gamma_R=\gamma_D=\sqrt{2}$ and has a gapless minimum at $k_+^0=\sqrt{2}/L_s$. As we move away from the symmetry point, a gap develops (dashed blue and green lines). How is the gap behaving as we vary the coupling parameters in the vicinity of the symmetry point? To answer this question, we define d_γ as the distance in the parameter space (γ_R,γ_D) from the symmetry point

$$d_\gamma=[(\gamma_R-\sqrt{2})^2+(\gamma_D-\sqrt{2})^2]^{1/2}. \tag{27}$$

If we move away from the symmetry point by changing the ratio between the Rashba and linear Dresselhaus interactions in the absence of a cubic Dressselhaus term, i.e., by varying the ratio α/β_1 and keeping $\beta_3=0$ (see the inset of Fig. 2, blue dashed line), the gap remains very small in comparison with the zero momentum frequency, $i\omega_2(0)\approx 2/\tau_s$. In contrast, the gap develops rapidly if we move along a direction in parameter space corresponding to $\gamma_R=\gamma_D$ (green/light gray line). This observation suggests that, in order to observe experimentally the "absence" of spin relaxation at a certain finite momentum, the minimization of the cubic Dresselhaus interaction should be a major concern. In addition, we have to remember the small momenta relaxation times given by Eqs. (25) and (26), in particular, the one associated with the $i\omega_1$ mode. To summarize the results concerning relaxation times, we refer to the diagram in Fig. 1. For a uniform system ($k=0$), the only mode that contributes to the dynamics is $i\omega_3$, and the corresponding spin-relaxation time of the out-of-plane component S_z is $\tau_s/2$, regardless of the spin-orbit coupling parameters. The system can have a slower relaxation at nonzero momenta that can be either arbitrarily small or of order $1/L_s$, depending on the values of the coupling parameters γ_R and γ_D. In the red region (zone I), all three modes $i\omega_j(\mathbf{k})$ have the minimum at $k=0$ and the largest spin-relaxation time, $\tau_{max}(0)=\tau_s/(1-|\gamma_R\gamma_D|/2)$, is obtained at small k vectors. In the blue/II (yellow/III) region, in addition to this small momentum minimum, we have the minima at k_+^0 (k_-^0) given by Eqs. (23) and (24), and to determine the slowest spin relaxation, we have to compare $\tau_{max}(0)$ with $\tau_{max}(k_\pm)=\tau_s/i\omega_{2(1)}(k_\pm^0)$. Finally, in the green regions (IV), the largest spin-relaxation time is associated with one of the minima at $k_\pm^0$. The diffusion is isotropic if $\gamma_R\gamma_D=0$ and anisotropic otherwise, especially in the vicinity of the symmetry points.

B. Real-space picture

We now turn our attention to the real-space behavior of D_{zz}, corresponding to the diffusion of a delta-function-like spin density injected in the origin at $t=0$. While the analytical treatment of the general case is rather complicated, we can easily solve special cases, such as the isotropic case ($\gamma_R\gamma_D=0$) or the symmetry point $\gamma_R=\pm\gamma_D=\sqrt{2}$. In particular, for the isotropic case we obtain from Eq. (11), after inverting the matrix and performing a Fourier transform with respect to the frequency,

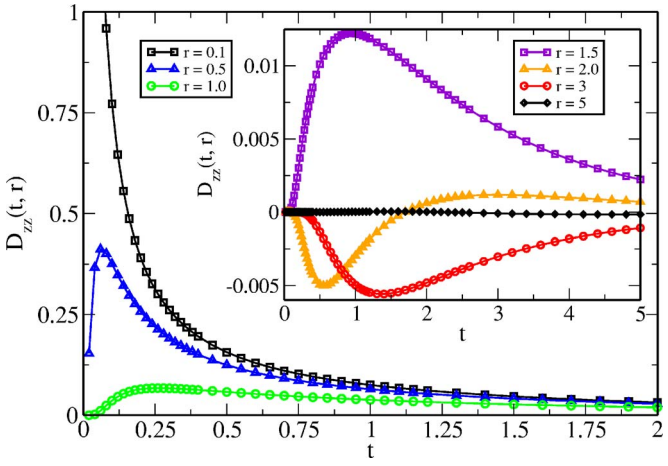

FIG. 3. (Color online) Relaxation of the out-of-plane spin density in the pure Rashba case. The spin density ρ_z, having an initial δ-like profile in real space, is injected in the origin at $t=0$. The curves show the time evolution $\rho_z(t,r)=D_{zz}(t,r)$ at various distances r from the origin. The large time behavior is described by Eq. (30) for $\gamma=2$. Time is expressed in units of τ_s and length in units of L_s.

$$D_{zz}(t,\mathbf{k})=\frac{1}{2}\left(1+\frac{1}{\sqrt{1+4\gamma^2k^2}}\right)e^{-(3/2+k^2+(1/2)\sqrt{1+4\gamma^2k^2})t}+\frac{1}{2}\left(1-\frac{1}{\sqrt{1+4\gamma^2k^2}}\right)e^{-(3/2+k^2-(1/2)\sqrt{1+4\gamma^2k^2})t}, \tag{28}$$

where $\gamma=\gamma_R$ if $\gamma_D=0$ and $\gamma=\gamma_D$ if we have a pure Dresselhaus spin-orbit coupling. The real-space dependence is obtained after performing another Fourier transform, with respect to momentum, which reduces to the one-dimensional integral

$$D_{zz}(t,\mathbf{r})=\frac{1}{4\pi}\int_0^\infty dk k J_0(kr)D_{zz}(t,\mathbf{k}), \tag{29}$$

where $J_0(kr)$ represents a Bessel function of the first kind. The time dependence of $D_{zz}(t,\mathbf{r})$ at distance r form the origin is shown in Fig. 3 for the particular case of pure Rashba coupling, $\gamma=2$. The curves represent the time evolution of the out-of-plane spin density at different positions in the plane after spin was injected in the origin at $t=0$. Notice the oscillations in the direction of the spin polarization (see Fig. 4). The analytical expressions for these oscillations can be derived in the large time limit using a saddle-point approximation for the integral over momenta [more precisely in the limit $t/\tau_s\gg(r/L_s)^2$]. For the isotropic case, this asymptotic behavior has the form

$$D_{zz}(t,\mathbf{r})\approx\frac{\gamma^2-1}{8\gamma\sqrt{\pi t}}J_0\left(\frac{\sqrt{\gamma^4-1}}{2\gamma}r\right)e^{-[(6\gamma^2-\gamma^4-1)/4\gamma^2]t}\quad\text{if } |\gamma|>1,$$

$$D_{zz}(t,\mathbf{r})\approx\frac{\gamma^2}{4\pi(1-\gamma^2)t^2}e^{-t}\quad\text{if } |\gamma|<1, \tag{30}$$

where $\gamma=\gamma_R$ or $\gamma=\gamma_D$, as appropriate. The asymptotic behavior is qualitatively different for $|\gamma_R|>1$ (or $|\gamma_D|>1$), the green regions (IV) in Fig. 1, and $|\gamma_R|<1$ (or $|\gamma_D|<1$), red zone (I). In the first case, $D_{zz}(t,\mathbf{r})$ oscillates in space at large distances away from the origin, $r/L_s \gg 1$, with a period $\lambda=2\pi/(L_s k^0)$ and an amplitude that decays as $\exp[-i\omega(k^0)t]/\sqrt{rt}$, where $k^0=k_+^0=k_-^0$ and $i\omega(k^0)=i\omega_1(k_-^0)=i\omega_2(k_+^0)$ are the parameters for the finite momentum minima of the dispersion relations described by Eqs. (23) and (24). By contrast, in the red region (I), spin diffusion at large times, $t/\tau_s \gg (r/L_s)^2$, is independent of position. In addition, the spin-relaxation time has the value τ_s, independent of the spin-orbit coupling, and the time dependence of the prefactor is $1/t^2$, instead of the $1/\sqrt{t}$ dependence for the oscillating case.

For $\gamma_R\gamma_D\neq 0$, the dynamics of the S_z spin component is anisotropic. The simplest analytical treatment of such a case obtains at the symmetry points $|\gamma_{R(D)}|=\sqrt{2}$. Starting with Eq. (13), we get, after inverting the matrix and performing a Fourier transform with respect to the frequency,

$$D_{zz}(t,\mathbf{k})=\frac{1}{2}e^{-[(\sqrt{2}+k_+)^2+k_-^2]t}+\frac{1}{2}e^{-[(\sqrt{2}-k_+)^2+k_-^2]t}, \quad (31)$$

where we assumed that $\gamma_R\gamma_D=2$, which corresponds to the symmetry points S_1 and S_1' in Fig. 1. A similar equation can be obtained for $\gamma_R\gamma_D=-2$ by exchanging k_+ and k_-. This equation does not acquire any spin-charge coupling corrections, as the coupling vanishes at the symmetry points, $\mu_0=\mu_1=0$, regardless of the strength of the spin-orbit interaction. Next, after performing the Fourier transform with respect to momentum, we obtain the exact real-space dependence at the symmetry point,

$$D_{zz}(t,\mathbf{r})=\frac{1}{4\pi t}e^{-r^2/4t}\cos(\sqrt{2}r_+), \quad (32)$$

where $r^2=r_+^2+r_-^2$ and we assumed that $\gamma_R\gamma_D=2$. Because of the gapless minimum of the $i\omega_2(k_+)$ mode, the large time decay is proportional to $1/t$, rather than exponential. In addition, the spin density oscillates along the r_+ direction due to the finite momentum minimum, while it becomes independent of r_- in the large time limit. For a general anisotropic case, the asymptotic behavior is determined by the minimum of the lowest relaxation rate. A characterization of the locations of the lowest minimum in the plane of the spin-orbit coupling parameters is provided in Fig. 5. We determine the asymptotic spin dynamics using a quadratic approximation for the dispersion curves in the vicinity of the minima. The approximate solutions of the secular equation $\Delta(s,\mathbf{k})$ for wave vectors with arbitrary k_+ and small k_- components are given in Appendix A. Assuming that $\gamma_R\gamma_D>0$, the zero momentum minimum of the $i\omega_1$ mode represents the lowest-energy contribution for a system with spin-orbit coupling parameters corresponding to the pink zone in Fig. 5. The asymptotic S_z spin diffusion in zone I of the parameter space (see Fig. 5) is described by

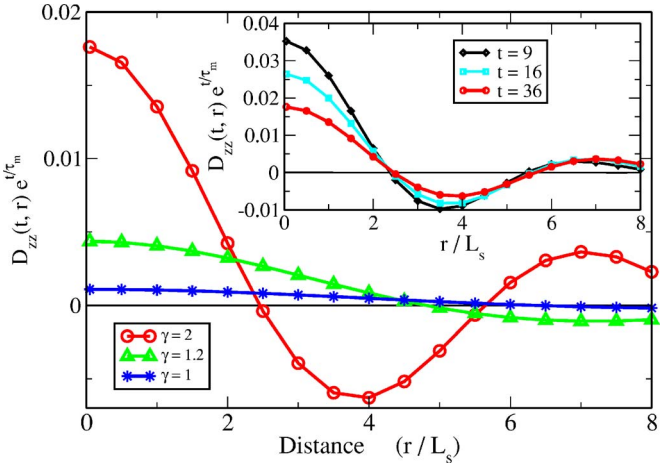

FIG. 4. (Color online) Real-space dependence of the out-of-plane spin density in a system with isotropic spin-orbit interaction. The curves represent $D_{zz}(t,r)$ multiplied by the exponential factor $\exp(t/\tau_m)$, where $t=36$ (in units of τ_s) and $\tau_m=(6\gamma^2-\gamma^4-1)/(4\gamma^2)$ represents the maximum relaxation time corresponding to the finite k^0 minimum of the relaxation rate. At short distances, $r\ll\sqrt{t}=6$, the solutions are described by Eq. (30). The period of the spatial oscillations increases as we decrease γ: $\gamma=2$ (pure Rashba or pure linear Dresselhaus interaction), red line and circles; $\gamma=1.2$, green line and triangles; $\gamma=1$, blue line and stars. Notice that, as we approach the nonoscillatory regime characterized by $\gamma<1$, the spin density becomes independent of distance in the asymptotic limit $t\gg r^2$ [see Eq. (30) and the $\gamma=1$ curve]. The inset shows the spatial dependence of the spin density of a pure Rashba system ($\gamma=2$) at different times. Again, we multiplied the results by the exponential factors $\exp(t/\tau_m)$. Notice that in the limit described by Eq. (30), the curves are proportional, with proportionality factors 1/3 (black curve and diamonds, $t=9$), 1/4 (cyan with squares, $t=16$), and 1/6 (red line and circles, $t=36$).

$$D_{zz}^{\mathrm{I}}(t,\mathbf{r})\approx\frac{2tC_0^{(1)}-r_-^2}{16\pi t^3}\frac{(\gamma_R-\gamma_D)^2}{\left(1+\frac{\gamma_R\gamma_D}{2}\right)^2(C_0^{(1)})^{5/2}}\times e^{-(1/4t)(r_+^2+r_-^2/C_0^{(1)})-(1-\gamma_R\gamma_D/2)t}, \quad (33)$$

where the coefficient $C_0^{(1)}$ is given by Eq. (A4). Equation (33) is valid for times larger than the spin-relaxation time, $t\gg\tau_s$, when $\gamma_R\neq\gamma_D$. When the couplings are equal, the $i\omega_1$ mode whose $k=0$ minimum generates the asymptotic behavior described by Eq. (33) does not contribute to the spin dynamics. Instead, for $\gamma_R=\gamma_D$ corresponding to the OP segment in Fig. 5, the lowest minimum is the zero momentum minimum of the $i\omega_2$ mode and it will generate an expression similar to Eq. (33), but with $r_\pm\to r_\mp$ and $\gamma_D\to-\gamma_D$. Notice that in this regime, spin diffusion is anisotropic only for times of order r^2 or smaller and becomes isotropic at longer times. Finally, for the anisotropic regime controlled by a finite momentum minimum in the dispersion relations, the blue and yellow regions and the segment PS_1 in Fig. 5, the asymptotic expression for D_{zz} can be obtained using the quadratic expansions given in Appendix A, in particular, Eqs. (A7) and (A8). We obtain the asymptotic expression for the diffuson in the

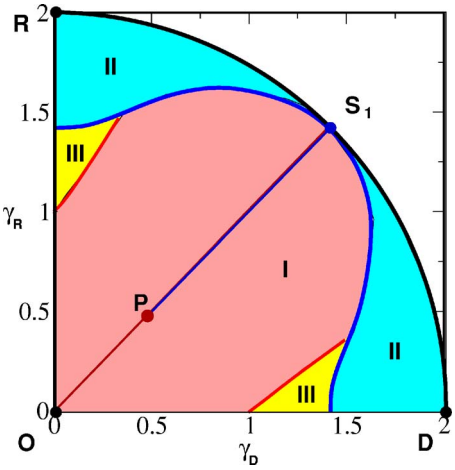

FIG. 5. (Color online) Diagram summarizing the asymptotic relaxation of the out-of-plane spin density in real space for a quarter of the parameter space ($\gamma_R \geqslant 0$, $\gamma_D \geqslant 0$). In the pink zone I (except the segment OS_1 corresponding to $\gamma_R = \gamma_D$), the solution is anisotropic at short times and becomes isotropic at large times. This solution is controlled by the zero momentum minimum $i\omega_1(0) = 1 - \gamma_R\gamma_D/2$ and has the asymptotic expression given by Eq. (33). For the segment OP, the solution is controlled by the zero momentum minimum $i\omega_2(0) = 1 + \gamma_R\gamma_D/2$ and has the same general characteristics as the neighboring pink zone. In the blue region II, the solution is anisotropic at all time scales and features real-space oscillations along the "+" direction. The long-time dynamics is controlled by the finite momentum minimum $i\omega_2(k_+^0)$ and the asymptotic behavior is described by Eq. (34). The same type of solution is valid for the PS_1 segment. Finally, in the yellow zone III, the solution has real-space oscillations along the "−" direction and an asymptotic behavior controlled by the finite momentum minimum $i\omega_1(k_-^0)$. Notice that, as we approach the axes $\gamma_R = 0$ and $\gamma_D = 0$, the spin relaxation, as described by Eq. (28), becomes isotropic. We stress that the regimes represented here are well defined in the long-time limit. At some intermediate time scales, and especially near the zone boundaries, the solution may exhibit mixed characteristics when the minima of two distinct relaxation rate modes have comparable contributions.

regime described by zone II of the parameter space (see Fig. 5),

$$\mathrm{D}_{zz}^{\mathrm{II}}(t,\mathbf{r}) \approx \frac{1}{4\pi t}\frac{D_{k_+^0}^{(2)}}{\sqrt{B_{k_+^0}^{(2)}C_{k_+^0}^{(2)}}} \times \exp\left[-\frac{1}{4t}\left(\frac{r_+^2}{B_{k_+^0}^{(2)}} + \frac{r_-^2}{C_{k_+^0}^{(2)}}\right) - i\omega_2(k_+^0)t\right]\cos(k_+^0 r_+), \tag{34}$$

where $D_{k_+^0}^{(2)} = 1 - (1 - \gamma_R\gamma_D/2)/(\gamma_R + \gamma_D)^2$, $B_{k_+^0}^{(2)}$ and $C_{k_+^0}^{(2)}$ are given in Appendix A, and $i\omega_2(k_+^0)$ represents the k_+^0 minimum of the $i\omega_2$ mode given explicitly by Eqs. (23) and (24). Equation (34) describes the large time dynamics of the out-of-plane spin component when the $i\omega_2(k_+^0)$ represents the lowest-energy minimum, i.e., for the blue zone and the segment PS_1 in Fig. 5. A similar expression can be obtained when the dynamics is controlled by the $i\omega_1(k_-^0)$ minimum (yellow zone III) using the correspondence rules $i\omega_2 \to i\omega_1$, $r_+ \leftrightarrow r_-$, and $\gamma_D \to -\gamma_D$:

$$\mathrm{D}_{zz}^{\mathrm{III}}(t,\mathbf{r}) \approx \frac{1}{4\pi t}\frac{D_{k_-^0}^{(2)}}{\sqrt{B_{k_-^0}^{(2)}C_{k_-^0}^{(2)}}} \times \exp\left[-\frac{1}{4t}\left(\frac{r_-^2}{B_{k_-^0}^{(2)}} + \frac{r_+^2}{C_{k_-^0}^{(2)}}\right) - i\omega_1(k_-^0)t\right]\cos(k_-^0 r_-), \tag{35}$$

where $D_{k_-^0}^{(2)} = 1 - (1 + \gamma_R\gamma_D/2)/(\gamma_R - \gamma_D)^2$ and the coefficients $B_{k_-^0}^{(2)}$ and $C_{k_-^0}^{(2)}$ are given in Appendix A. Notice that Eqs. (34) and (35) reduce to Eq. (31) at the symmetry points $\gamma_R = \gamma_D = \pm\sqrt{2}$ where it becomes exact. Within this regime, the solution of the diffusion equation is characterized by real-space oscillations with a period $\lambda = 2\pi L_s/k_+^0$ determined by the position of the minimum in k space, while at times much larger than $\tau_s r^2/L_s^2$, the solution becomes independent of r_-. The relaxation time, $\tau_s/[i\omega_2(k_+^0)]$, can be much larger than the relaxation time in the regime controlled by the zero momentum minimum, $\tau_s/[i\omega_1(0)]$, and diverges as we approach the symmetry points. On the other hand, when we approach the $\gamma_R = 0$ or $\gamma_D = 0$ axes, the solution becomes isotropic and some of the approximations used in deriving Eqs. (33) and (34) are no longer valid. Instead, the asymptotic behavior in the isotropic regime is described by Eq. (30).

IV. THE ROLE OF THE SPIN-CHARGE COUPLING

In this section, we study the effects of spin-charge coupling on spin and charge diffusion. The main results of this section are Eqs. (37) and (42) describing the behavior of the relaxation rate modes in the presence of the spin-charge coupling.

In the absence of spin-charge coupling, the charge diffuses according to the standard diffusion equation, while a spin density characterized by a given k vector decays, in general, as a sum of three exponentials. Recent spin-grating experiments[24] have shown that, in certain conditions, the time decay of an optically injected spin density may include an oscillatory component. In this section, we explore the possibility that the appearance of these oscillations is due to spin-charge coupled dynamics. To this end, we rederive Green's function of the diffusion equation starting from the polarizability matrix [Eq. (11)], or from Eq. (13), but without neglecting the spin-charge coupling terms proportional to μ_0 and μ_1. Inverting the polarizability matrix produces, in general, a complicated expression for the diffuson. However, there are several special cases in which significant simplifications occur. These cases involve, on the one hand, special values of the spin-orbit coupling parameters, namely, the pure Rashba interaction, $\gamma_D = 0$, $\gamma_R = \pm 2$, the pure Dresselhaus coupling, $\gamma_R = 0$, and the symmetry points $\gamma_R = \pm\sqrt{2}$, $\gamma_D = \pm\sqrt{2}$. On the other hand, the inversion of $\Pi(\omega,\mathbf{k})$ can be performed analytically for *arbitrary* values of the spin-orbit

coupling parameters along the special directions in momentum space corresponding to k_+ and k_-. Our strategy is to obtain explicit analytical expressions for these special cases and use them, in conjunction with numerical results for arbitrary sets of parameters, to extract and characterize the main features of the general solution. We start with the isotropic case corresponding to a pure Rashba coupling, or a pure Dresselhaus spin-orbit interaction. The modes that control the coupled spin-charge dynamics are the solutions of the secular equation

$$\Delta(s,\mathbf{k}) \equiv [s(s+1) - \gamma^2 k^2][s(s-1) + g^2\mu_l^2 k^2] = 0, \quad (36)$$

where $\Delta(s,\mathbf{k})$ is the determinant of the $\hat{\Pi}(s,\mathbf{k})$ matrix, $s=-i\omega+1+k^2$, and $\gamma=\pm 2$ for the Rashba case or $\gamma=\gamma_D\in[-2,2]$ for a pure Dresselhaus spin-orbit interaction. The spin-charge coupling is measured by the parameter μ_l and we have $\mu_l=\mu_1=\text{sign}(\alpha)\alpha^2$ in the Rashba case and $\mu_l=\mu_0=[(3\beta_3-\beta_1)(\beta_3^2-\beta_1^2)-\beta_1\beta_3^2]/[(\beta_1-\beta_3)^2+\beta_3^2]^{1/2}$ for the Dresselhaus coupling. The full expression of the diffusion matrix is given in Appendix B. The real-time behavior of the diffusion propagator can be obtained after performing a Fourier transform of Eq. (B1) with respect to the frequency. This time dependence is determined by the roots $s_j=-i\omega_j+1+k^2$ of Eq. (36) and has the general form (17). For the pure cases described by the Eqs. (36) and (B1), the four modes that control the coupled spin-charge dynamics are

$$\begin{aligned} i\omega_0(\mathbf{k}) &= \tfrac{1}{2} + k^2 - \tfrac{1}{2}\sqrt{1-4g^2\mu_l^2k^2}, \\ i\omega_1(\mathbf{k}) &= \tfrac{1}{2} + k^2 + \tfrac{1}{2}\sqrt{1-4g^2\mu_l^2k^2}, \\ i\omega_2(\mathbf{k}) &= \tfrac{3}{2} + k^2 - \tfrac{1}{2}\sqrt{1+4\gamma^2k^2}, \\ i\omega_3(\mathbf{k}) &= \tfrac{3}{2} + k^2 + \tfrac{1}{2}\sqrt{1+4\gamma^2k^2}, \end{aligned} \quad (37)$$

where $g=2v_Fk_F\tau$, $k^2=k_x^2+k_y^2$, and the k vector is expressed, as usual, in units of $1/L_s$. Equation (37) has several key features. First, we notice that the mode responsible for the charge dynamics in the absence of spin-charge coupling, namely $i\omega_0$, couples with only one spin mode, $i\omega_1$, while the other spin modes, $i\omega_2$ and $i\omega_3$, remain unaffected by the spin-charge coupling. Consequently, the modes $i\omega_2$ and $i\omega_3$ are real and positive for any value of the momentum, and the corresponding terms in Eq. (17) will decay exponentially with time. On the other hand, the solutions $i\omega_0$ and $i\omega_1$ are real only if $2g\alpha^2k_FL_s=2\pi v_Fk_F\alpha<1$. This condition is always satisfied in the weak spin-orbit coupling regime, in which the diffusion equation formalism applies. We conclude that within the diffusive regime, a system will never exhibit oscillatory dynamics. Below, we show that this conclusion holds for arbitrary spin-orbit coupling parameters. Nonetheless, we can formally extrapolate Eq. (37) outside its strict domain of validity and apply it to the strong spin-orbit interaction regime. In this limit, i.e., for $\pi v_Fk_F\alpha>1$, the modes $i\omega_0$ and $i\omega_1$ acquire an imaginary component, which generates oscillatory terms in the solution (17). We interpret this second major feature of Eq. (37) as an indication that oscillatory dynamics is a signature of strong spin-orbit interactions. While the diffusion equation formalism cannot offer a quantitative description of this regime, it should represent a good indicator for the range of parameters where the oscillatory behavior is likely to appear and for the degree in which various components of the spin and charge sectors are affected. For example, from Eq. (B1), we observe that the time evolution of the diagonal S_z component D_{zz} is controlled by the modes $i\omega_2$ and $i\omega_3$, which do not couple with the charge. Consequently, in the pure Rashba (or pure Dresselhaus) case, the out-of-plane spin component does not exhibit oscillatory dynamics for any strength of the spin-orbit coupling. This result is connected to the isotropic nature of the spin-orbit splitting in these particular cases. In contrast, the dynamics of the in-plane spin components is coupled with the charge dynamics. Explicitly, the time dependence of the matrix element D_{00} describing charge relaxation is given by

$$D_{00}(t,\mathbf{k}) = \begin{cases} \left[\cosh\left(\frac{t}{2}\sqrt{1-4g^2\mu_l^2k^2}\right) + \frac{\sinh\left(\frac{t}{2}\sqrt{1-4g^2\mu_l^2k^2}\right)}{\sqrt{1-4g^2\mu_l^2k^2}}\right]e^{-(1/2+k^2)t} & \text{if } 2g\mu_lk<1 \\ \left[\cos\left(\frac{t}{2}\sqrt{4g^2\mu_l^2k^2-1}\right) + \frac{\sin\left(\frac{t}{2}\sqrt{4g^2\mu_l^2k^2-1}\right)}{\sqrt{4g^2\mu_l^2k^2-1}}\right]e^{-(1/2+k^2)t} & \text{if } 2g\mu_lk>1, \end{cases} \quad (38)$$

where the wave vector k is expressed in units of $1/L_s$ and time in units of spin-relaxation time τ_s. Notice that in the absence of spin-charge coupling, D_{00} reduces to the standard solution of the diffusion equation, $D_{00}(t,\mathbf{k})=\exp(-k^2t)$, while the time dependence of the matrix elements associated with the spin degrees of freedom is determined by s_2 and s_3 only. This behavior is illustrated in Fig. 6, which shows the time dependence of all diagonal matrix elements $\hat{D}_{ii}(t,\mathbf{k})$ for

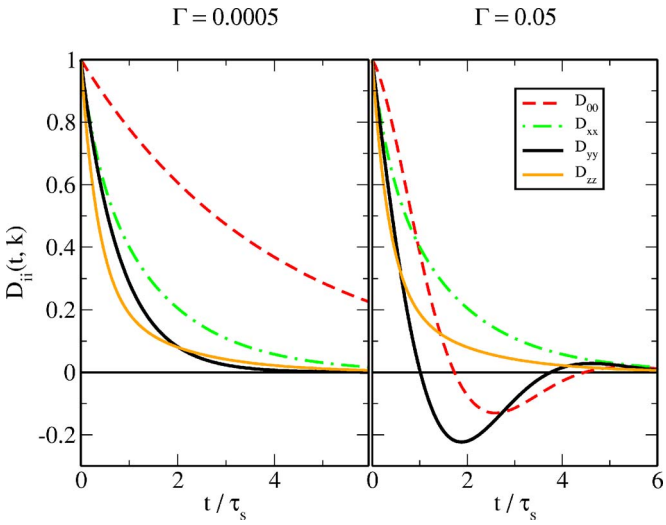

FIG. 6. (Color online) Time dependence of the diagonal components of the diffusion matrix in the weak spin-orbit coupling (left panel) and strong spin-orbit coupling (right panel) regimes. The matrix elements are evaluated for the pure Rashba case ($\gamma_R=2$, $\gamma_D=0$) at a momentum $(k_x,k_y)=(0.5/L_s,0)$. In the weak spin-orbit coupling limit, all the quantities decay exponentially, while in the opposite limit, the charge and the S_y channels exhibit oscillatory behavior. In the pure Rashba (or pure Dresselhaus) case, the out-of-plane spin component does not couple to the charge due to symmetry. For **k** parallel to the x axis, this is also the case for the in-plane S_x spin component [see Eq. (B1)].

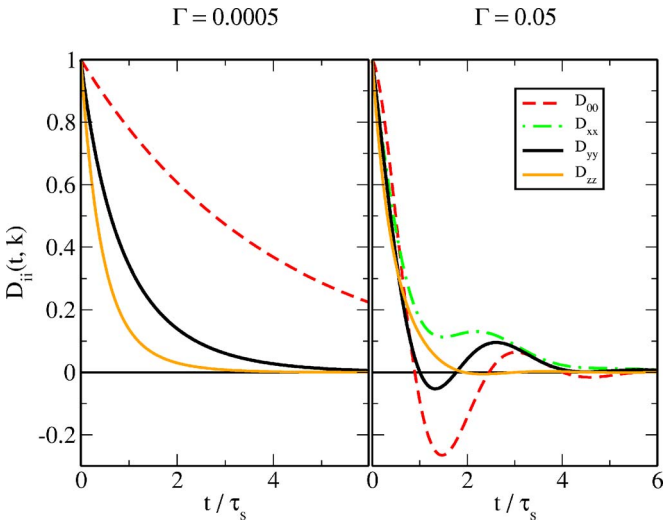

FIG. 7. (Color online) Time dependence of the diagonal components of the diffusion matrix in the weak spin-orbit coupling (left panel) and strong spin-orbit coupling (right panel) regimes for $\gamma_R=1=-\gamma_D$. The matrix elements are evaluated at a momentum $(k_x,k_y)=(0.5/L_s0)$. In the weak spin-orbit coupling limit, all the quantities decay exponentially, while in the opposite limit, they exhibit oscillatory behavior. Notice that due to the particular choice of parameters, in the weak-coupling limit, the in-plane spin components have identical relaxation curves, $D_{xx}=D_{yy}$, while in the strong-coupling limit, the two quantities differ due to the k-dependent coupling to the charge channel.

$\mathbf{k}=(0.5,0)$. The curves in the left panel were calculated in the weak spin-orbit coupling regime corresponding to $\Gamma=0.0005$ and $g=1000$. Notice that in the charge channel we have the standard exponential decay, $\exp(-k^2t)$, while in the spin channels the effect of the finite relaxation time $\tau_x=\tau_y=\tau_z/2$ is evident. By contrast, in the strong-coupling limit, the charge and S_y channels exhibit oscillatory behavior. Also notice that, as a result of the spin-charge coupling, the charge relaxes on the same time scale as the spin degrees of freedom. We mentioned above that for a pure Rashba (or pure Dresselhaus) spin-orbit coupling, the charge does not couple with the out-of-plane spin component due to symmetry. In the example shown in Fig. 6, similar symmetry reasons apply to the S_x spin component due to the particular choice of momentum along the x axis. However, in general, all spin components will couple to the charge. For example, the general expression for the D_{0z} matrix element describing the coupling between charge and out-of-plane spin density is

$$D_{0z}(s,\mathbf{k}) = \frac{g}{2\Delta(s,\mathbf{k})}(k_x^2-k_y^2)[\gamma_R\gamma_D(\gamma_D\mu_0-\gamma_R\mu_1) + 2s(\gamma_D\mu_1-\gamma_R\mu_0)], \tag{39}$$

where $\Delta(s,\mathbf{k})$ is the determinant of $\hat{D}^{-1}$. Let us consider a set of parameters for which D_{0z} is nonzero. We show in Fig. 7 the time dependence of the diagonal matrix elements in the presence of both Rashba and Dresselhaus terms, so that $\gamma_R=1$ and $\gamma_D=-1$. In terms of the original coupling constants, this case corresponds to $\alpha\approx 0.47\Gamma$, $\beta_1\approx 0.19\Gamma$, and $\beta_3\approx 0.66\Gamma$. Notice that in the strong-coupling limit (right panel in Fig. 7), all channels exhibit oscillatory behavior, although the relative amplitude for the S_z component is very small. Again, we observe that D_{00} decays on a time scale of order τ_s, instead of the standard exponential decay $\exp(-k^2t)$. We conclude that strong spin-orbit interaction can generate two effects: (1) an oscillatory structure in the decay curves and (2) an increase in the decay rate of the charge channel. The first effect should be observable above a certain critical momentum of order $k_c\approx g\mu_i/L_s$. The second effect can be understood as a renormalization of the diffusion constant. In the limit of small momenta, Eq. (38) reduces to

$$D_{00}(t,\mathbf{k}) \approx \exp[-(1+2g^2\mu_l^2)k^2t].$$

Consequently, in this limit the charge diffuses at long length scales according to the standard diffusion equation but with a renormalized diffusion constant. This effective diffusion constant is enhanced by a factor $1+2g^2\mu_l^2$ over its bare value:

$$\mathcal{D}_c^{\text{eff}} \approx (1+2g^2\mu_l^2)\frac{v_F^2\tau}{2}. \tag{40}$$

Formally, the enhancement factor can be very large. However, we have to remember that these conclusions are based on an extrapolation of the diffusion equation formalism outside its domain of validity and, therefore, should be seen as having qualitative rather than quantitative relevance. Strictly speaking, in the strong spin-orbit coupling regime, the diffusion equation formalism breaks down and the notion of a diffusion coefficient becomes meaningless. The coupled

spin-orbit dynamics is no longer described by a set of differential equations of type (11) and (13).

Our calculation using the diffusion equation formalism indicates that oscillatory dynamics may appear in a system with strong spin-orbit interaction as a consequence of spin-charge coupling. The effective strength of this coupling depends not only on the overall strength of the spin-orbit interaction, i.e., on Γ, but also on the interplay between different types of spin-orbit couplings. The net result of these competing effects is contained in the expressions of the spin-charge coupling coefficients μ_0 and μ_1 given by Eq. (12). In the examples considered above (see Figs. 6 and 7), we have $(\mu_0,\mu_1)=(0,\Gamma^2)$ for the pure Rashba case and $(\mu_0,\mu_1)=(1.09\Gamma^2,1.40\Gamma^2)$ for the $\gamma_R=1=-\gamma_D$ case. For comparison, the maximum values of the spin-charge coupling coefficients are $|\mu_0|\approx 1.10\Gamma^2$ and $|\mu_1|\approx 1.65\Gamma^2$. However, for other values of the spin-orbit coupling parameters, these coefficients, and implicitly the spin-charge coupling effects, may be much weaker. In particular, the special case corresponding to the symmetric points defined by $\gamma_R=\gamma_D=\pm\sqrt{2}$ deserves special attention (similar considerations can be made for the case $\gamma_R=-\gamma_D$ by interchanging the "+" and "−" components). In this case, $\mu_0=\mu_1=0$ and, consequently, the spin-charge coupling vanishes. Using the rotated coordinate system and expression (13) for the polarizability matrix, we obtain for the diffuson

$$\hat{D}^{(r)}(\omega,\mathbf{k})=\begin{pmatrix} \frac{1}{s-1} & 0 & 0 & 0 \\ 0 & \frac{s+1}{(s+1)^2-8k_+^2} & 0 & \frac{2\sqrt{2}ik_+}{(s+1)^2-8k_+^2} \\ 0 & 0 & \frac{1}{s-1} & 0 \\ 0 & \frac{-2\sqrt{2}ik_+}{(s+1)^2-8k_+^2} & 0 & \frac{s+1}{(s+1)^2-8k_+^2} \end{pmatrix}. \tag{41}$$

The effects of the spin-charge coupling are totally absent at the symmetry points, regardless of the strength of the spin-orbit interaction. In addition, the diffusion matrix is independent of the k_- wave-vector component and has a gapless mode for $k_+=\pm\sqrt{2}$, as discussed in the previous section.

To understand the effects of spin-orbit coupling in a system with arbitrary spin-orbit interaction, we calculate the diffusion matrix corresponding to wave vectors along the $k_\pm$ directions. From Eq. (13), we obtain the general expression for the matrix $\hat{D}^{(r)}(s,k_\pm)$ given in Appendix B. The real-time behavior can be obtained by Fourier transforming Eq. (B2) with respect to the frequency. Each matrix element has a time dependence of the form given by Eq. (17), except that this time the k vector is restricted to the $k_\pm$ directions. The four modes that control the coupled spin-charge dynamics are

$$\begin{aligned} i\omega_0(k_+)&=\frac{1}{2}+k_+^2-\frac{\gamma_R\gamma_D}{4}-\frac{1}{2}\sqrt{\left(1-\frac{\gamma_R\gamma_D}{2}\right)^2-4g^2(\mu_0+\mu_1)^2k_+^2}, \\ i\omega_1(k_+)&=\frac{1}{2}+k_+^2-\frac{\gamma_R\gamma_D}{4}+\frac{1}{2}\sqrt{\left(1-\frac{\gamma_R\gamma_D}{2}\right)^2-4g^2(\mu_0+\mu_1)^2k_+^2}, \\ i\omega_2(k_+)&=\frac{3}{2}+k_+^2+\frac{\gamma_R\gamma_D}{4}-\frac{1}{2}\sqrt{\left(1-\frac{\gamma_R\gamma_D}{2}\right)^2+4(\gamma_R+\gamma_D)^2k_+^2}, \\ i\omega_3(k_+)&=\frac{3}{2}+k_+^2+\frac{\gamma_R\gamma_D}{4}+\frac{1}{2}\sqrt{\left(1-\frac{\gamma_R\gamma_D}{2}\right)^2+4(\gamma_R+\gamma_D)^2k_+^2}, \end{aligned} \tag{42}$$

where μ_0 and μ_1 are expressed in terms of the spin-orbit coupling parameters in Eq. (12). Similar expressions can be written for the k_- direction, using the correspondence rules $+\rightarrow-$, $\gamma_D\rightarrow-\gamma_D$, $\mu_1\rightarrow-\mu_1$, and $i\omega_1\leftrightarrow i\omega_2$. As in the isotropic case discussed above, the charge mode $i\omega_0$ couples with only one spin mode, $i\omega_1$ for the k_+ direction and $i\omega_2$ for the k_- direction, while the other spin modes remain unaffected by the spin-charge coupling. Also, for these special k-space directions, the dynamics of the out-of-plane component of the spin is determined by the spin modes that do not couple to the charge; i.e., D_{zz} in Eq. (B2) depends on $i\omega_2(k_+)$ and $i\omega_3(k_+)$ only. We conclude that oscillatory dynamics, the renormalization of the diffusion constants, or any other spin-charge coupling effect should not be observable in the relaxation of an injected out-of-plane spin density with a wave vector along the $k_\pm$ directions. However, for an arbitrary di-

rection, the effects of the spin-charge coupling are present, as we have seen in Fig. 7, as all the modes contribute to the spin dynamics. The set of four relaxation rate modes has some main qualitative features that are independent of direction: (i) there are always at least two purely real modes, one of them being $i\omega_3$, and (ii) an imaginary component may be acquired by the charge mode $i\omega_0$ and one of the spin modes $i\omega_1$ or $i\omega_2$, exactly which one of them depending on the direction in k space. The appearance of the imaginary component takes place above a certain minimum value of the wave vector satisfying the condition $2g|\mu_0 \pm \mu_1|k_{min} = 1 \mp \gamma_R\gamma_D/2$. We mention that the existence of such an imaginary component does not necessarily generate an oscillatory relaxation of the spin and charge densities. The general solution in this case contains two exponentially decaying terms, in addition to the oscillatory term with exponentially decaying amplitude, and the existence of an oscillatory component in the relaxation curves is determined by the relative intensity of these contributions. Finally, at small values of the wave vector, the coupled spin-charge relaxation is always monotonic. However, the relaxation is, in general, anisotropic and the diffusion coefficients get renormalized.

V. SUMMARY

In this paper, we studied spin diffusion in a generic spin-orbit coupled system. We found that there are a number of different dynamic regimes and phenomena controlled by the relative values of the spin-orbit coupling parameters. These unusual phenomena include an enhancement of the spin polarization lifetime at finite wave vectors, anisotropic spin diffusion, an oscillatory behavior of the spin relaxation in real space, an enhancement of the effective charge diffusion coefficient, and possible real-time oscillations in spin diffusion dynamics. The existence and manifestations of these phenomena depend in a nontrivial manner on the strength of the various terms contributing to the spin-orbit interaction.

One of the main results of the paper is a general analytic form of the spin-charge coupled diffusion equation in the presence of all possible types of spin-orbit couplings. The parameters of this equation can be conveniently parametrized by three dimensionless coupling constants: the overall strength of the spin-orbit coupling (Γ) and two Rashba-type (γ_R) and Dresselhaus-type (γ_D) contributions to spin precession. The last two parameters must satisfy the physical constraint $\gamma_R^2 + \gamma_D^2 \leq 4$. We showed that spin diffusion can be completely characterized by the pair of these dimensionless parameters (γ_R, γ_D). We have identified the domains in the parameter space characterized by either nonzero or zero k-vector maxima of the spin-relaxation spectrum, which determine the asymptotic dynamics at large times. One particularly important example we considered is the vicinity of the symmetry point $|\gamma_R| = |\gamma_D| = \sqrt{2}$, where the lifetime becomes arbitrarily long for certain finite k vectors. Our analysis showed that, in order to observe this slow spin relaxation experimentally, special attention should be paid to minimize the cubic Dresselhaus spin-orbit interaction.

We have also qualitatively considered the regime of strong spin-charge coupling and extrapolated the results of the diffusion equation formalism to the strong spin-orbit interaction regime. We found that the enhancement of the charge diffusion coefficient and the oscillatory spin relaxation observed in recent spin-grating experiments can be qualitatively understood as a spin-charge coupling effect. We showed that the coupling of spin and charge is, in general, strongly k dependent and can be characterized by two parameters, μ_0 and μ_1, which depend on the spin-orbit interaction. These coupling parameters depend not only on the overall interaction strength Γ but also on the interplay between the Rashba and Dresselhaus contributions. We argued that a necessary condition to observe an oscillatory behavior is a strong spin-orbit interaction, corresponding to the crossover from diffusive transport to the ballistic regime. For a given direction in k space, the effect should be observable for k larger than a certain minimum wave vector. However, we predict that the effect is not observable along certain directions in k space for which spin-charge coupling is prevented by symmetry. For example, the out-of-plane spin polarization does not couple with the charge sector in the pure Rashba or pure Dresselhaus case. The coupling is also absent, in general, for directions in k space corresponding to k_+ and k_- (see text). In addition, we predict that the effect is absent if the competition between the Rashba and Dresselhaus terms generates small coupling constants μ_0 and μ_1, regardless of the overall strength of the spin-orbit interaction. This is the case, for example, in the vicinity of the special symmetry points where μ_0 and μ_1 vanish. We should reiterate here that the diffusion approximation may capture spin-charge coupled dynamics only qualitatively if the spin-charge coupling is strong. To obtain a quantitative theory in this case, one should study the dynamics of the matrix distribution functions in the Boltzmann equation.

APPENDIX A: SOLUTION OF THE SPIN DIFFUSION EQUATION IN THE LIMIT OF SMALL k_- WAVE NUMBERS

The secular equation $\Delta(s,\mathbf{k})=0$ has simple analytical solutions if one of the wave vector components k_- or k_+ vanishes. The asymptotic real-time and real-space spin dynamics is controlled by the minima of the dispersion curves $i\omega_j(\mathbf{k})$ that are either at zero momentum or at a finite value along the k_+ or k_- directions. To determine this asymptotic behavior, we need the solution of the secular equation in the vicinity of the minima. Assuming that k_- is small, we obtain for an arbitrary value of k_+ the following approximate solutions of the secular equation:

$$s_1(\mathbf{k}) = \frac{\gamma_R\gamma_D}{2} - \xi_1(k_+)k_-^2 + \mathcal{O}(k_-^4),$$

$$s_{2,3}(\mathbf{k}) = -\frac{1}{2} - \frac{\gamma_R\gamma_D}{4} \pm \frac{1}{2}\sqrt{\left(1 - \frac{\gamma_R\gamma_D}{2}\right)^2 + 4k_+^2(\gamma_R + \gamma_D)^2} - \xi_{2,3}(k_+)k_-^2 + \mathcal{O}(k_-^4), \tag{A1}$$

where the coefficients of the quadratic contributions in k_- are

$$\xi_1(k_+) = \frac{(\gamma_R - \gamma_D)^2}{\frac{(\gamma_R + \gamma_D)^2}{\gamma_R \gamma_D} k_+^2 - \left(1 + \frac{\gamma_R \gamma_D}{2}\right)},$$

$$\xi_{2,3}(k_+) = -\frac{\xi_1(k_+)}{2} \mp \frac{(\gamma_R - \gamma_D)^2 + \xi_1(k_+)\left(\frac{1}{2} + \frac{3}{4}\gamma_R \gamma_D\right)}{\sqrt{\left(1 - \frac{\gamma_R \gamma_D}{2}\right) + 4k_+^2(\gamma_R + \gamma_D)^2}}. \quad \text{(A2)}$$

Similar expressions can be obtained for wave vectors with small k_+ and arbitrary k_- components using the correspondence rules $s_1 \leftrightarrow s_2$, $k_+ \leftrightarrow k_-$ and $\gamma_D \rightarrow -\gamma_D$. We notice that this quadratic approximation is valid away from level crossing points. For example, the denominator of ξ_1 vanishes for a set of parameters corresponding to a degeneracy point for the $i\omega_1$ and $i\omega_2$ modes.

The quadratic expansion around the $\mathbf{k}=0$ minimum of the $i\omega_1$ mode has the form

$$i\omega_1(\mathbf{k}) = 1 - \frac{\gamma_R \gamma_D}{2} + k_+^2 + C_0^{(1)}(\gamma_R, \gamma_D) k_-^2 + \mathcal{O}(k^4), \quad \text{(A3)}$$

with

$$C_0^{(1)}(\gamma_R, \gamma_D) = 1 - \frac{(\gamma_R - \gamma_D)^2}{1 + \frac{\gamma_R \gamma_D}{2}}. \quad \text{(A4)}$$

This zero momentum minimum exists provided $C_0^{(1)} \times (\gamma_R, \gamma_D) > 0$, i.e., for spin-orbit coupling parameters corresponding to the red and blue zones in Fig. 1, but it does not contribute to the dynamics along the line with equal Rashba and Dresselhaus couplings, $\gamma_R = \gamma_D$. Similarly, we obtain for the zero momentum minimum of the $i\omega_2$ mode that exists within the red and yellow regions in Fig. 1 the expression

$$i\omega_2(\mathbf{k}) = 1 + \frac{\gamma_R \gamma_D}{2} + k_-^2 + C_0^{(2)}(\gamma_R, \gamma_D) k_+^2 + \mathcal{O}(k^4), \quad \text{(A5)}$$

with

$$C_0^{(2)}(\gamma_R, \gamma_D) = 1 - \frac{(\gamma_R + \gamma_D)^2}{1 - \frac{\gamma_R \gamma_D}{2}}. \quad \text{(A6)}$$

For the finite momentum minimum of the $i\omega_2$ mode at k_+^0 that exists within the blue and green zones (see Fig. 1) we obtain from Eqs. (A1) and (A2)

$$i\omega_2(\mathbf{k}) \approx \frac{3}{2} + \frac{\gamma_R \gamma_D}{4} - \frac{\left(1 - \frac{\gamma_R \gamma_D}{2}\right)^2}{4(\gamma_R + \gamma_D)^2} - \frac{(\gamma_R + \gamma_D)^2}{4} + B_{k_+^0}^{(2)}(k_+ - k_+^0)^2 + C_{k_+^0}^{(2)} k_-^2, \quad \text{(A7)}$$

where the coefficients of the quadratic terms are

$$B_{k_+^0}^{(2)}(\gamma_R, \gamma_D) = 1 - \frac{\left(1 - \frac{\gamma_R \gamma_D}{2}\right)^2}{(\gamma_R + \gamma_D)^4},$$

$$C_{k_+^0}^{(2)}(\gamma_R, \gamma_D) = 1 - \frac{(\gamma_R - \gamma_D)^2}{(\gamma_R + \gamma_D)^2} \frac{\gamma_R^2 + \gamma_D^2 + \frac{5}{2}\gamma_R \gamma_D - 1}{\gamma_R^2 + \gamma_D^2 + \frac{1}{2}\gamma_R \gamma_D - 1}. \quad \text{(A8)}$$

Similar expressions can be obtained for the finite momentum minimum of the $i\omega_1$ mode, corresponding to the yellow and green regions in Fig. 1, using the correspondence rules $i\omega_2 \rightarrow i\omega_1$, $k_+ \leftrightarrow k_-$, and $\gamma_D \rightarrow -\gamma_D$.

APPENDIX B: EXPLICIT EXPRESSIONS OF THE DIFFUSION MATRIX IN THE PRESENCE OF SPIN-CHARGE COUPLING

The diffusion matrix propagator for pure Rashba or pure Dresselhaus spin-orbit interaction can be obtained by inverting the polarizability matrix from Eq. (11), after setting $\gamma_D = 0$ and $\mu_0 = 0$ (for the Rashba case) or $\gamma_R = 0$ and $\mu_1 = 0$ (for Dresselhaus spin-orbit interaction). We obtain

$$\hat{D}(\omega, \mathbf{k}) = \begin{pmatrix} \frac{s}{(s-s_0)(s-s_1)} & \frac{ig\mu_l k_y}{(s-s_0)(s-s_1)} & \frac{-ig\mu_l k_x}{(s-s_0)(s-s_1)} & 0 \\ \frac{ig\mu_l k_y}{(s-s_0)(s-s_1)} & \frac{s(s^2-1) - (s-1)\gamma^2 k_y^2 + (s+1)g^2\mu_l^2 k_x^2}{\Delta(s,\mathbf{k})} & \frac{k_x k_y((s-1)\gamma^2 + (s+1)g^2\mu_l^2)}{\Delta(s,\mathbf{k})} & \frac{i\gamma k_x}{(s-s_2)(s-s_3)} \\ \frac{-ig\mu_l k_x}{(s-s_0)(s-s_1)} & \frac{s(s^2-1) - (s-1)\gamma^2 k_y^2 + (s+1)g^2\mu_l^2 k_x^2}{\Delta(s,\mathbf{k})} & \frac{s(s^2-1) - (s-1)\gamma^2 k_x^2 + (s+1)g^2\mu_l^2 k_y^2}{\Delta(s,\mathbf{k})} & \frac{i\gamma k_y}{(s-s_2)(s-s_3)} \\ 0 & \frac{-i\gamma k_x}{(s-s_2)(s-s_3)} & \frac{-i\gamma k_y}{(s-s_2)(s-s_3)} & \frac{s}{(s-s_2)(s-s_3)} \end{pmatrix}, \quad \text{(B1)}$$

where $\gamma = \pm 2$ for the Rashba interaction and $\gamma \in [-2, 2]$ for the Dresselhaus case, the spin-charge coupling parameter is given

by Eq. (12), and $\Delta(s,\mathbf{k})=(s-s_0)(s-s_1)(s-s_2)(s-s_3)$ is the determinant of the polarizability matrix. The solutions of the secular equation $\Delta=0$ are $s_j(\mathbf{k})=-i\omega_j(\mathbf{k})+1+k^2$ with the dispersion relations for the modes $i\omega_j$ given by Eq. (37).

For a general set of spin-orbit interaction parameters, one can easily invert the matrix in Eq. (13) and obtain the diffuson matrix for wave vectors oriented along the "+" and "−" axes of the rotated coordinate system. Explicitly, for the k_+ direction we have

$$\hat{D}(\omega,k_+)=\begin{pmatrix} \dfrac{s-\dfrac{\gamma_R\gamma_D}{2}}{(s-s_0)(s-s_1)} & 0 & \dfrac{-ig(\mu_0+\mu_1)k_+}{(s-s_0)(s-s_1)} & 0 \\ 0 & \dfrac{s+1}{(s-s_2)(s-s_3)} & 0 & \dfrac{-i(\gamma_R+\gamma_D)k_+}{(s-s_2)(s-s_3)} \\ \dfrac{-ig(\mu_0+\mu_1)k_+}{(s-s_0)(s-s_1)} & 0 & \dfrac{s-1}{(s-s_0)(s-s_1)} & 0 \\ 0 & \dfrac{i(\gamma_R+\gamma_D)k_+}{(s-s_2)(s-s_3)} & 0 & \dfrac{s+\dfrac{\gamma_R\gamma_D}{2}}{(s-s_2)(s-s_3)} \end{pmatrix}, \tag{B2}$$

where $s_j=-i\omega_j+1+k_+^2$ represent the four modes described by Eq. (42). Notice that the charge couples only with the S_- spin component, i.e., with the in-plane component perpendicular to the wave vector. A similar expression can be obtained for the k_- direction using the standard correspondence rules $+\leftrightarrow-$ and $\gamma_D\rightarrow-\gamma_D$.

[1] *Semiconductor Spintronics and Quantum Computing*, edited by D. D. Awschalom, D. Loss, and N. Samarth (Springer, New York, 2002).
[2] D. Loss and D. P. DiVincenzo, Phys. Rev. A **57**, 120 (1998).
[3] J. Nitta, T. Akazaki, H. Takayanagi, and T. Enoki, Phys. Rev. Lett. **78**, 1335 (1997).
[4] D. Grundler, Phys. Rev. Lett. **84**, 6074 (2000).
[5] Y. Kato, R. C. Myers, A. C. Gossardand, and D. D. Awschalom, Nature (London) **427**, 50 (2004).
[6] S. Murakami, N. Nagaosa, and S.-C. Zhang, Science **301**, 1348 (2003).
[7] J. Sinova, D. Culcer, Q. Niu, N. A. Sinitsyn, T. Jungwirth, and A. H. MacDonald, Phys. Rev. Lett. **92**, 126603 (2004).
[8] T. Koga, J. Nitta, H. Takayanagi, and S. Datta, Phys. Rev. Lett. **88**, 126601 (2002).
[9] I. Žutić, J. Fabian, and S. Das Sarma, Rev. Mod. Phys. **76**, 323 (2004).
[10] S. A. Wolf, D. D. Awschalom, R. A. Buhrmanand, J. M. Daughton, S. von Molnar, M. L. Roukes, A. Y. Chtchelkanova, and D. M. Treger, Science **294**, 1488 (2001).
[11] E. I. Rashba, Sov. Phys. Solid State **2**, 1109 (1960).
[12] Yu. A. Bychkov and E. I. Rashba, J. Phys. C **17**, 6093 (1984).
[13] G. Dresselhaus, Phys. Rev. **100**, 580 (1955).
[14] M. I. Dyakonov and V. Yu. Kachorovskii, Sov. Phys. Semicond. **20**, 110 (1986).
[15] G. Bergmann, Phys. Rep. **107**, 1 (1984).
[16] W. Knap, C. Skierbiszewski, A. Zduniak, E. Litwin-Staszewska, D. Bertho, F. Kobbi, J. L. Robert, G. E. Pikus, F. G. Pikus, S. V. Iordanskii, V. Mosser, K. Zekentes, and Yu. B. Lyanda-Geller, Phys. Rev. B **53**, 3912 (1996).
[17] F. J. Jedema, A. T. Filip, and B. J. van Wees, Nature (London) **410**, 345 (2001).
[18] H.-A. Engel, B. I. Halperin, and E. I. Rashba, Phys. Rev. Lett. **95**, 166605 (2005).
[19] S. D. Ganichev, E. L. Ivchenko, V. V. Belkov, S. A. Tarasenko, M. Sollinger, D. Weiss, W. Wegscheider, and W. Prettl, Nature (London) **417**, 153 (2002).
[20] M. I. Dyakonov and V. I. Perel, Sov. Phys. JETP **33**, 1053 (1971); Phys. Lett. **35A**, 459 (1971).
[21] J. B. Miller, D. M. Zumbuhl, C. M. Marcus, Y. B. Lyanda-Geller, D. Goldhaber-Gordon, K. Campman, and A. C. Gossard, Phys. Rev. Lett. **90**, 076807 (2003).
[22] S. Giglberger, L. E. Golub, V. V. Belkov, S. N. Danilov, D. Schuh, Ch. Gerl, F. Rohlfing, J. Stahl, W. Wegscheider, D. Weiss, W. Prettl, and S. D. Ganichev, cond-mat/0609569 (to be published).
[23] A. R. Cameron, P. Riblet, and A. Miller, Phys. Rev. Lett. **76**, 4793 (1996).
[24] C. P. Weber, N. Gedik, J. E. Moore, J. Orenstein, J. Stephens, and D. D. Awschalom, Nature (London) **437**, 1330 (2005).
[25] C. P. Weber, J. Orenstein, B. A. Bernevig, S.-C. Zhang, J. Stephens, and D. D. Awschalom, cond-mat/0610054 (to be published).
[26] S. A. Crooker and D. L. Smith, Phys. Rev. Lett. **94**, 236601 (2005).
[27] M. Hruska, S. Kos, S. A. Crooker, A. Saxena, and D. L. Smith, Phys. Rev. B **73**, 075306 (2006).
[28] G. D. Mahan, *Many-Particle Physics* (Plenum, New York, 1981).
[29] A. A. Burkov, A. S. Nunez, and A. H. MacDonald, Phys. Rev. B **70**, 155308 (2004).
[30] A. G. Malshukov and K. A. Chao, Phys. Rev. B **71**, 121308(R) (2005).

[31] A. G. Malshukov, L. Y. Wang, C. S. Chu, and K. A. Chao, Phys. Rev. Lett. **95**, 146601 (2005).
[32] A. V. Shytov, E. G. Mishchenko, H.-A. Engel, and B. I. Halperin, Phys. Rev. B **73**, 075316 (2006).
[33] V. A. Froltsov, Phys. Rev. B **64**, 045311 (2001).
[34] N. S. Averkiev and L. E. Golub, Phys. Rev. B **60**, 15582 (1999).
[35] B. A. Bernevig, J. Orenstein, and S.-C. Zhang, Phys. Rev. Lett. **97**, 236601 (2006).